Zn2SnO4-Based Photoelectrodes for Organolead Halide Perovskite Solar Cells

ARTICLE *in* THE JOURNAL OF PHYSICAL CHEMISTRY C · OCTOBER 2014

Impact Factor: 4.77 · DOI: 10.1021/jp509183k

THE JOURNAL OF PHYSICAL CHEMISTRY C

Article

pubs.acs.org/JPCC

Zn_2SnO_4-Based Photoelectrodes for Organolead Halide Perovskite Solar Cells

Lee Seul Oh,[†,‡,▽] Dong Hoe Kim,[§,▽] Jin Ah Lee,[†] Seong Sik Shin,[§] Jin-Wook Lee,[∥] Ik Jae Park,[†,§] Min Jae Ko,[†] Nam-Gyu Park,[∥] Sung Gyu Pyo,*[,⊥] Kug Sun Hong,[§] and Jin Young Kim*[,†,#]

[†]Photo-electronic Hybrids Research Center, Korea Institute of Science and Technology (KIST), Seoul 136-791, Korea

[‡]Department of Chemical Engineering and Materials Science, Chung-Ang University, Seoul 156-756, Korea

[§]Department of Materials Science and Engineering, Seoul National University, Seoul 151-742, Korea

[∥]School of Chemical Engineering and Department of Energy Science, Sungkyunkwan University, Suwon 440-746, Korea

[⊥]School of Integrative Engineering, Chung-Ang University, Seoul 156-756, Korea

[#]Green School, Korea University, Seoul 136-701, Korea

Supporting Information

ABSTRACT: We report a new ternary Zn_2SnO_4 (ZSO) electron-transporting electrode of a $CH_3NH_3PbI_3$ perovskite solar cell as an alternative to the conventional TiO_2 electrode. The ZSO-based perovskite solar cells have been prepared following a conventional procedure known as a sequential (or two-step) process with ZSO compact/mesoscopic layers instead of the conventional TiO_2 counterparts, and their solar cell properties have been investigated as a function of the thickness of either the ZSO compact layer or the ZSO mesoscopic layer. The presence of the ZSO compact layer has a negligible influence on the transmittance of the incident light regardless of its thickness, whereas the thickest compact layer blocks the back-electron transfer most efficiently. The open-circuit voltage and fill factor increase with the increasing thickness of the mesoscopic ZSO layer, whereas the short-circuit current density decreases with the increasing thickness except for the thinnest one (~100 nm). As a result, the device with a 300 nm-thick mesoscopic ZSO layer shows the highest conversion efficiency of 7%. In addition, time-resolved and frequency-resolved measurements reveal that the ZSO-based perovskite solar cell exhibits faster electron transport (~10 times) and superior charge-collection capability compared to the TiO_2-based counterpart with similar thickness and conversion efficiency.

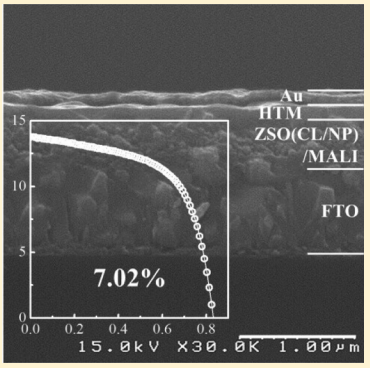

Organolead-halide-based hybrid solar cells (or perovskite solar cells) are being spotlighted a lot in recent years as a new highly efficient solid-state thin film solar cell.[1−11] The structure of the first perovskite solar cell stems from the dye-sensitized solar cell (DSSC), where the Ru-based or organic dye sensitizers have been replaced with the organolead halide perovskites such as $CH_3NH_3PbI_3$ (methylammonium lead iodide; MALI).[1,12] Afterward, some structural variations such as the mesoscopic heterojunction structure,[13,14] planar heterojunction structure,[15,16] and the incorporation of p-/n-type organic semiconductors[3,17−19] have been reported. In terms of the fabrication technique, most of the mesostructured devices have been prepared via either single-step[1,2] or two-step[8] solution processes, whereas the devices with planar structures have been fabricated through either the solution process[9,16,20] or the thermal evaporation.[15] In spite of the diverse structural variations, the sensitizer type that incorporates a mesoscopic TiO_2 electron-transporting layer is still one of the widely investigated device structures.

Ternary oxide materials have attracted significant attention in the DSSC area as an alternative electron-transporting phase to the conventional TiO_2, because their electronic/optical properties can be easily controlled by manipulating the composition and/or by doping. For instance, we have recently reported ternary oxides such as $BaSnO_3$ and Zn_2SnO_4 (ZSO) as an electron-transporting material of the DSSC, where the new oxide materials have been found to exhibit decent device performances.[21,22] Among the ternary oxide systems, the ZSO-based photoanode is particularly promising, as the charge injection from the sensitizer and the electron diffusion through the nanoparticle network are significantly faster than the TiO_2-based photoanode.[22]

In this study, we report the first use of the ternary ZSO nanoparticles as an electron-transporting material of the perovskite solar cell. The effects of the ZSO compact/mesoscopic layers on the solar cell properties of the ZSO-based perovskite solar cells have been investigated, and the electron dynamics of the ZSO-based perovskite solar cell has been compared to the conventional TiO_2-based counterpart. The perovskite solar cells have been fabricated via the two-step process,[8] and the detailed experimental procedure is described

Received: September 11, 2014
Published: September 26, 2014

   dx.doi.org/10.1021/jp509183k | J. Phys. Chem. C 2014, 118, 22991−22994

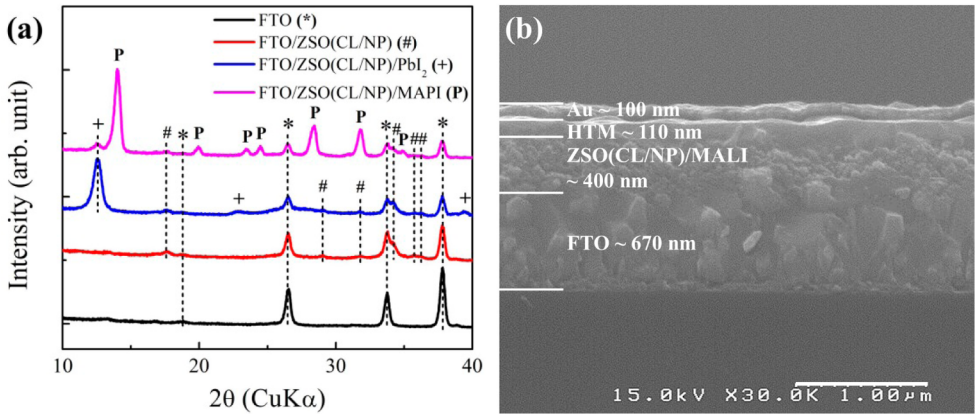

Figure 1. (a) X-ray diffraction patterns of the samples at various preparation steps and (b) a typical cross-sectional SEM image of a ZSO-based perovskite solar cell.

in the Supporting Information. Briefly, a ZSO or TiO_2 compact layer was deposited on a patterned FTO substrate using a spin coating method, and then a diluted ZSO or TiO_2 nanoparticle paste was spin-coated to form a mesoscopic ZSO or TiO_2 layer. After annealing the oxide film, a PbI_2/oxide film was prepared by spin-coating a PbI_2-containing dimethylformamide (DMF) solution, followed by dipping in a methylammonium iodide solution to form the MALI/oxide film. Then, a hole-transporting layer (spiro-OMeTAD) and a current-collecting layer (Au) were deposited using spin coating and thermal evaporation, respectively.

Figure 1a presents the evolution of the crystallographic structure during the fabrication procedure of the ZSO-based perovskite solar cell, where the diffraction peaks from the FTO substrate (JCPDS no. 46-1088), ZSO compact/mesoscopic layers (JCPDS no. 74-2184), PbI_2 (JCPDS no. 07-0235), and MALI are denoted by '*', "#", '+', and "P", respectively. Most of the peaks in the X-ray diffraction pattern of the MALI/ZSO film can be assigned to those from MALI, ZSO, or FTO except for a small peak at 12.56° which is from the unreacted (or decomposed) PbI_2. Figure 1b displays a typical cross-sectional scanning electron microscopy (SEM) image. Stacked layers of the ZSO-based perovskite solar cell consisting of an FTO substrate (~670 nm), ZSO compact layer (~100 nm), mesoscopic ZSO particle film filled with MALI (~300 nm), hole-transporting material (HTM; spiro-OMeTAD, ~ 110 nm), and Au (~100 nm) can be clearly observed in the SEM image.

It has been found from our preliminary experiments that the use of the ZSO compact layer as opposed to the conventional TiO_2 compact layer is crucial for having the ZSO-based perovskite solar cells work properly owing to the electron-blocking effect resulting from the higher conduction band edge position of TiO_2 compared to ZSO (Figure S1), which is consistent with our previous work on ZSO-based DSSCs.[22] It was also found that coating the ZSO compact layers does not influence the optical transmittance of the FTO substrate (Figure S2) because their refractive indexes are the same.[22] After investigating the blocking layer effect with various ZSO compact layer thickness (Figure S3), the optimal thickness of 110 nm has been selected. Figure 2 shows the dependence of the solar cell parameters of the ZSO-based perovskite solar cells on the thickness of the mesoscopic ZSO layer, which is also summarized in Table 1. The solar cell parameters are averaged from around 10 different cells. The thickness of the mesoscopic

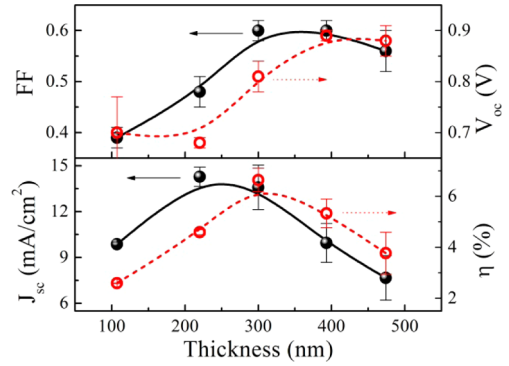

Figure 2. *J*–*V* characteristics of ZSO-based solar cells as a function of the ZSO film thickness.

Table 1. Solar Cell Parameters of ZSO-Based Perovskite Solar Cells with Various Film Thickness, Where the Values Are Averaged from ~10 Cells for Each Thickness

thickness (nm)	J_{sc} (mA/cm^2)	V_{oc} (V)	fill factor	efficiency (%)
107	9.87 (±0.13)	0.70 (±0.07)	0.39 (±0.02)	2.59 (±0.01)
220	14.28 (±0.63)	0.68 (±0.01)	0.48 (±0.03)	4.59 (±0.10)
300	13.58 (±1.45)	0.81 (±0.03)	0.60 (±0.02)	6.64 (±0.46)
393	9.95 (±1.28)	0.89 (±0.01)	0.60 (±0.02)	5.33 (±0.56)
474	7.66 (±1.45)	0.88 (±0.03)	0.56 (±0.04)	3.77 (±0.82)

ZSO layer could be controlled from 100 to 500 nm simply by varying the speed of the spin coating process (Figure S4). The open-circuit voltage (V_{oc}) and fill factor show increasing trends with the increasing ZSO thickness. The small fill factor and low V_{oc} of the devices with thin ZSO layers can be ascribed to the better chance of direct contact between spiro-OMeTAD and the substrate when the mesoscopic layers are too thin, which can lead to the decreased shunt resistance. The short-circuit current density (J_{sc}) increases with the ZSO thickness up to 220 nm, and then monotonically decreases. The amount of the active material (i.e., MALI) is probably too small for the thinnest ZSO layer, resulting in the initial increase of J_{sc}. The smaller J_{sc} with the thicker nanoparticle layer is commonly observed for the MALI-based perovskite solar cells,[1] which is generally associated with the poor charge collection with the thicker layer.[23] As a result of the compromise among the solar cell parameters, the ZSO-based perovskite solar cells exhibit the

dx.doi.org/10.1021/jp509183k | J. Phys. Chem. C 2014, 118, 22991–22994

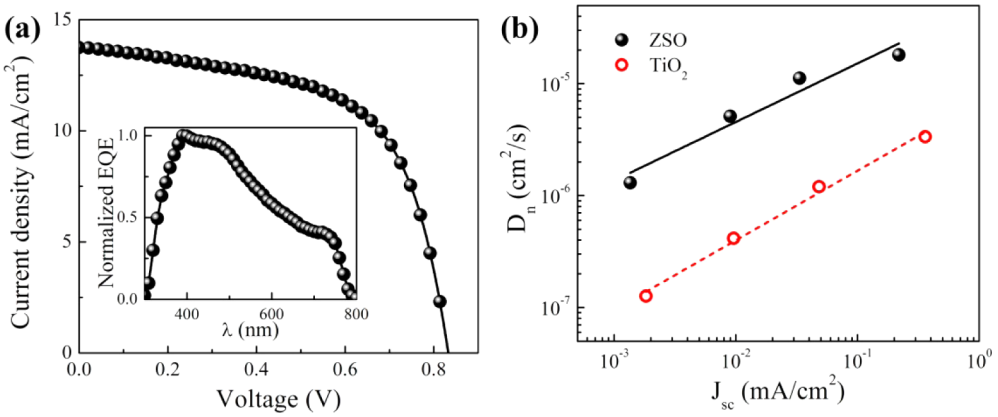

Figure 3. (a) J–V curve (and a normalized external quantum efficiency curve) and (b) electron diffusion coefficients of the ZSO-based perovskite solar cell with the highest conversion efficiency. Electron diffusion coefficients of a TiO_2-based perovskite solar cell with similar thickness (~300 nm) and conversion efficiency (~7%) are also presented for a comparison.

highest conversion efficiency when the thickness of the mesoscopic ZSO layer is 300 nm.

Figure 3a displays the current density–voltage (J–V) curve of the best ZSO-based perovskite solar cell with a 300 nm of mesoscopic ZSO layer, where the inset shows the normalized external quantum efficiency (EQE) curve. The J_{sc}, V_{oc}, fill factor, and the conversion efficiency of the best ZSO-based perovskite solar cell are 13.78 mA/cm^2, 0.83 V, 61.4%, and 7.02%, respectively. When compared with one of the highest TiO_2-based perovskite solar cell with similar device geometry and synthetic procedure ($J_{sc} \approx 20$ mA/cm^2, $V_{oc} \approx 1$ V, FF ≈ 70%, $\eta \approx 14\%$),[24] the J_{sc}, V_{oc}, and the fill factor are smaller by 31%, 17%, and 12%, respectively, resulting in the 50% deficit in the conversion efficiency. The smaller J_{sc} can be understood from the spectral photoresponse (i.e., EQE curve) as shown in the inset of Figure 3a. The photoresponse or the external quantum efficiency in the longer wavelength region (λ > 500 nm) is significantly lower compared to that in the shorter wavelength region (λ < 500 nm). In general, the poor photoresponse in the longer wavelength region or near the band edge can be ascribed to the poor collection or significant recombination of the photoelectrons or holes generated near the back contact owing to the weaker absorption of the small energy photons by the absorber material.[25,26] The poor red responses can also be ascribed to the small amount of the absorber material or the insufficient formation of the MALI overlayer on top of the mesoscopic ZSO layer because of the same wavelength-dependent absorption issue. The smaller V_{oc} can result from the conduction band edge position of ZSO, which is lower by ~200 mV compared to TiO_2.[22] Based on our experience, however, the effect of the conduction band position on the V_{oc} becomes weaker when the electron-transporting phase (i.e., ZSO) is physically separated from the HTM (i.e., spiro-OMeTAD) by forming a complete MALI overlayer between them. Therefore, the formation of the uniform MALI overlayer on top of the mesoscopic ZSO layer via the processing optimization can lead to the increased J_{sc} and V_{oc}. Figure 3b shows the electron diffusion coefficients of the best ZSO-based perovskite solar cell under various light intensities (i.e., J_{sc}), where those of the TiO_2-based counterpart with similar film thickness (~300 nm) and conversion efficiency (~7%) are displayed together for comparison. The solid/dotted lines represent best fit of the data. Both of the ZSO- and TiO_2-based perovskite solar cells exhibit typical power-law dependence of the electron diffusion coefficient on J_{sc} (i.e., photoelectron density) as observed for other perovskite solar cells[23,27] and DSSCs.[21,28] In the whole range of J_{sc}, the ZSO-based perovskite solar cell exhibits about 10-times larger electron diffusion coefficient than the TiO_2-based counterpart. This result is very consistent with our previous study on the ZSO-based DSSCs with the iodide-based electrolyte, where the ZSO showed about 10-times larger diffusion coefficient than TiO_2.[22] The frequency-dependent time-resolved photoresponse measurements (Figure S5) also revealed that the ZSO-based perovskite solar cell shows superior charge-collecting capability compared to the TiO_2-based counterpart, which is in consistent with its larger diffusion coefficient. The faster electron diffusion in the mesoscopic oxide layer can be particularly beneficial for the perovskite solar cells in terms of the balanced electron/hole mobility, given the geometric similarity to the bulk-heterojunction solar cells.[29]

In summary, we have successfully demonstrated the first use of the ternary ZSO nanoparticles as an electron-transporting material of the perovskite solar cell. The V_{oc} and fill factor of the ZSO-based perovskite solar cell increased with the increasing thickness of the mesoscopic ZSO layer, whereas the J_{sc} decreased with the increasing thickness except for the thinnest one. As a result, the ZSO-based perovskite solar cell with 300 nm thick ZSO layer showed the best performance of 7.02%, which can be further improved by optimizing the fabrication procedure. In addition, the ZSO-based perovskite solar cell exhibited faster electron diffusion by 10 times and superior charge collection compared to the TiO_2-based counterpart with similar device performance, which is very promising as an alternative to the conventional TiO_2 system.

■ ASSOCIATED CONTENT

Supporting Information

Experimental details, J–V curves, UV–vis spectroscopy, SEM, Transient photoresponse measurements. This material is available free of charge via the Internet at http://pubs.acs.org.

■ AUTHOR INFORMATION

Corresponding Authors

*E-mail: sgpyo@cau.ac.kr.

*Tel: +82-2-958-5368. E-mail: kimjy@kist.re.kr.

Author Contributions

$^{\nabla}$Authors contributed equally.

Author Contributions

The manuscript was written through contributions of all authors. All authors have given approval to the final version of the manuscript.

Notes

The authors declare no competing financial interest.

■ ACKNOWLEDGMENTS

The work done at KIST was supported by the KIST internal fund, Nano•Material Technology Development Program through the National Research Foundation of Korea (NRF) funded by the Ministry of Science, ICT & Future Planning (2012M3A7B4049989), and the "National Agenda Project" program of Korea Research Council of Fundamental Science & Technology (KRCF). The work done at Green School was supported by the National Research Foundation of Korea Grant funded by the Korean Government (MSIP) (2013, University-Institute cooperation program).

■ REFERENCES

(1) Kim, H.-S.; Lee, C.-R.; Im, J.-H.; Lee, K.-B.; Moehl, T.; Marchioro, A.; Moon, S.-J.; Humphry-Baker, R.; Yum, J.-H.; Moser, J. E.; Grätzel, M.; Park, N.-G. Lead Iodide Perovskite Sensitized All-Solid-State Submicron Thin Film Mesoscopic Solar Cell with Efficiency Exceeding 9%. *Sci. Rep.* **2012**, *2*, 591.

(2) Lee, M. M.; Teuscher, J.; Miyasaka, T.; Murakami, T. N.; Snaith, H. J. Efficient Hybrid Solar Cells Based on Meso-Superstructured Organometal Halide Perovskites. *Science* **2012**, *338*, 643−647.

(3) Heo, J. H.; Im, S. H.; Noh, J. H.; Mandal, T. N.; Lim, C.-S.; Chang, J. A.; Lee, Y. H.; Kim, H.-j.; Sarkar, A.; NazeeruddinMd, K.; Grätzel, M.; Seok, S. I. Efficient Inorganic-Organic Hybrid Heterojunction Solar Cells Containing Perovskite Compound and Polymeric Hole Conductors. *Nat. Photonics* **2013**, *7*, 486−491.

(4) Xing, G.; Mathews, N.; Sun, S.; Lim, S. S.; Lam, Y. M.; Grätzel, M.; Mhaisalkar, S.; Sum, T. C. Long-Range Balanced Electron- and Hole-Transport Lengths in Organic-Inorganic $CH_3NH_3PbI_3$. *Science* **2013**, *342*, 344−347.

(5) Bi, D.; Yang, L.; Boschloo, G.; Hagfeldt, A.; Johansson, E. M. J. Effect of Different Hole Transport Materials on Recombination in $CH_3NH_3PbI_3$ Perovskite-Sensitized Mesoscopic Solar Cells. *J. Phys. Chem. Lett.* **2013**, *4*, 1532−1536.

(6) Stranks, S. D.; Eperon, G. E.; Grancini, G.; Menelaou, C.; Alcocer, M. J. P.; Leijtens, T.; Herz, L. M.; Petrozza, A.; Snaith, H. J. Electron-Hole Diffusion Lengths Exceeding 1 Micrometer in an Organometal Trihalide Perovskite Absorber. *Science* **2013**, *342*, 341−344.

(7) Docampo, P.; Ball, J. M.; Darwich, M.; Eperon, G. E.; Snaith, H. J. Efficient Organometal Trihalide Perovskite Planar-Heterojunction Solar Cells on Flexible Polymer Substrates. *Nat. Commun.* **2013**, *4*, 2761.

(8) Burschka, J.; Pellet, N.; Moon, S.-J.; Humphry-Baker, R.; Gao, P.; Nazeeruddin, M. K.; Grätzel, M. Sequential Deposition as a Route to High-Performance Perovskite-Sensitized Solar Cells. *Nature* **2013**, *499*, 316−319.

(9) Liu, D.; Kelly, T. L. Perovskite Solar Cells with a Planar Heterojunction Structure Prepared using Room-Temperature Solution Processing Techniques. *Nat. Photonics* **2014**, *8*, 133−138.

(10) Dharani, S.; Mulmudi, H. K.; Yantara, N.; Thu Trang, P. T.; Park, N. G.; Graetzel, M.; Mhaisalkar, S.; Mathews, N.; Boix, P. P. High Efficiency Electrospun TiO_2 Nanofiber Based Hybrid Organic-Inorganic Perovskite Solar Cell. *Nanoscale* **2014**, *6*, 1675−1679.

(11) Qin, P.; Domanski, A. L.; Chandiran, A. K.; Berger, R.; Butt, H.-J.; Dar, M. I.; Moehl, T.; Tetreault, N.; Gao, P.; Ahmad, S.; Nazeeruddin, M. K.; Grätzel, M. Yttrium-Substituted Nanocrystalline TiO_2 Photoanodes for Perovskite Based Heterojunction Solar Cells. *Nanoscale* **2014**, *6*, 1508−1514.

(12) Kojima, A.; Teshima, K.; Shirai, Y.; Miyasaka, T. Organometal Halide Perovskites as Visible-Light Sensitizers for Photovoltaic Cells. *J. Am. Chem. Soc.* **2009**, *131*, 6050−6051.

(13) Etgar, L.; Gao, P.; Xue, Z.; Peng, Q.; Chandiran, A. K.; Liu, B.; Nazeeruddin, M. K.; Grätzel, M. Mesoscopic $CH_3NH_3PbI_3/TiO_2$ Heterojunction Solar Cells. *J. Am. Chem. Soc.* **2012**, *134*, 17396−17399.

(14) Laban, W. A.; Etgar, L. Depleted Hole Conductor-Free Lead Halide Iodide Heterojunction Solar Cells. *Energy Environ. Sci.* **2013**, *6*, 3249−3253.

(15) Liu, M.; Johnston, M. B.; Snaith, H. J. Efficient Planar Heterojunction Perovskite Solar Cells by Vapour Deposition. *Nature* **2013**, *501*, 395−398.

(16) Chen, Q.; Zhou, H.; Hong, Z.; Luo, S.; Duan, H.-S.; Wang, H.-H.; Liu, Y.; Li, G.; Yang, Y. Planar Heterojunction Perovskite Solar Cells via Vapor-Assisted Solution Process. *J. Am. Chem. Soc.* **2013**, *136*, 622−625.

(17) Jeng, J.-Y.; Chiang, Y.-F.; Lee, M.-H.; Peng, S.-R.; Guo, T.-F.; Chen, P.; Wen, T.-C. $CH_3NH_3PbI_3$ Perovskite/Fullerene Planar-Heterojunction Hybrid Solar Cells. *Adv. Mater.* **2013**, *25*, 3727−3732.

(18) Sun, S.; Salim, T.; Mathews, N.; Duchamp, M.; Boothroyd, C.; Xing, G.; Sum, T. C.; Lam, Y. M. The Origin of High Efficiency in Low-Temperature Solution-Processable Bilayer Organometal Halide Hybrid Solar Cells. *Energy Environ. Sci.* **2014**, *7*, 399−407.

(19) Abrusci, A.; Stranks, S. D.; Docampo, P.; Yip, H.-L.; Jen, A. K. Y.; Snaith, H. J. High-Performance Perovskite-Polymer Hybrid Solar Cells via Electronic Coupling with Fullerene Monolayers. *Nano Lett.* **2013**, *13*, 3124−3128.

(20) Eperon, G. E.; Burlakov, V. M.; Docampo, P.; Goriely, A.; Snaith, H. J. Morphological Control for High Performance, Solution-Processed Planar Heterojunction Perovskite Solar Cells. *Adv. Funct. Mater.* **2014**, *24*, 151−157.

(21) Shin, S. S.; Kim, J. S.; Suk, J. H.; Lee, K. D.; Kim, D. W.; Park, J. H.; Cho, I. S.; Hong, K. S.; Kim, J. Y. Improved Quantum Efficiency of Highly Efficient Perovskite $BaSnO_3$-Based Dye-Sensitized Solar Cells. *ACS Nano* **2013**, *7*, 1027−1035.

(22) Shin, S. S.; Kim, D. W.; Hwang, D.; Suk, J. H.; Oh, L. S.; Han, B. S.; Kim, D. H.; Kim, J. S.; Kim, D.; Kim, J. Y.; Hong, K. S. Controlled Interfacial Electron Dynamics in Highly Efficient Zn_2SnO_4-Based Dye-Sensitized Solar Cells. *ChemSusChem* **2014**, *7*, 501−509.

(23) Zhao, Y.; Zhu, K. Charge Transport and Recombination in Perovskite $(CH_3NH_3)PbI_3$ Sensitized TiO_2 Solar Cells. *J. Phys. Chem. Lett.* **2013**, *4*, 2880−2884.

(24) Lee, J.-W.; Lee, T.-Y.; Yoo, P. J.; Gratzel, M.; Mhaisalkar, S.; Park, N.-G. Rutile TiO_2-Based Perovskite Solar Cells. *J. Mater. Chem. A* **2014**, *2*, 9251−9259.

(25) Kim, J. Y.; Noh, J. H.; Zhu, K.; Halverson, A. F.; Neale, N. R.; Park, S.; Hong, K. S.; Frank, A. J. General Strategy for Fabricating Transparent TiO_2 Nanotube Arrays for Dye-Sensitized Photoelectrodes: Illumination Geometry and Transport Properties. *ACS Nano* **2011**, *5*, 2647−2656.

(26) Jeon, J.-O.; Lee, K. D.; Seul Oh, L.; Seo, S.-W.; Lee, D.-K.; Kim, H.; Jeong, J.-h.; Ko, M. J.; Kim, B.; Son, H. J.; Kim, J. Y. Highly Efficient Copper-Zinc-Tin-Selenide (CZTSe) Solar Cells by Electrodeposition. *ChemSusChem* **2014**, *7*, 1073−1077.

(27) Zhao, Y.; Nardes, A. M.; Zhu, K. Solid-State Mesostructured Perovskite $CH_3NH_3PbI_3$ Solar Cells: Charge Transport, Recombination, and Diffusion Length. *J. Phys. Chem. Lett.* **2014**, *5*, 490−494.

(28) van de Lagemaat, J.; Frank, A. J. Nonthermalized Electron Transport in Dye-Sensitized Nanocrystalline TiO_2 Films: Transient Photocurrent and Random-Walk Modeling Studies. *J. Phys. Chem. B* **2001**, *105*, 11194−11205.

(29) Liu, Z.; Liu, Q.; Huang, Y.; Ma, Y.; Yin, S.; Zhang, X.; Sun, W.; Chen, Y. Organic Photovoltaic Devices Based on a Novel Acceptor Material: Graphene. *Adv. Mater.* **2008**, *20*, 3924−3930.